

Article

Not peer-reviewed version

GIS-AHP-Based Site Suitability Assessment for Green Hydrogen Production: A Case Study of Luderitz, Namibia

[Ernesto T. O. Samuel](#), [Tom Wanjekeche](#)^{*}, [Andreas Ndapuka](#)

Posted Date: 2 February 2026

doi: 10.20944/preprints202602.0019.v1

Keywords: AHP; green hydrogen; GIS; optimization; solar PV; wind farm



Preprints.org is a free multidisciplinary platform providing preprint service that is dedicated to making early versions of research outputs permanently available and citable. Preprints posted at Preprints.org appear in Web of Science, Crossref, Google Scholar, Scilit, Europe PMC.

Copyright: This open access article is published under a [Creative Commons CC BY 4.0 license](#), which permit the free download, distribution, and reuse, provided that the author and preprint are cited in any reuse.

Disclaimer/Publisher's Note: The statements, opinions, and data contained in all publications are solely those of the individual author(s) and contributor(s) and not of MDPI and/or the editor(s). MDPI and/or the editor(s) disclaim responsibility for any injury to people or property resulting from any ideas, methods, instructions, or products referred to in the content.

Article

GIS-AHP-Based Site Suitability Assessment for Green Hydrogen Production: A Case Study of Luderitz, Namibia

Ernesto T.O. Samuel, Tom Wanjekeche * and Andreas Ndapuka

Department of Electrical and Computer Engineering, University of Namibia, Ongwediva, Namibia

* Correspondence: twanjekeche@unam.na

Abstract

Namibia's vast renewable energy potential positions it as a strategic location for green hydrogen production, a key vector in advancing global decarbonization objectives. Nevertheless, identifying optimal production sites remains a complex and multidimensional challenge. This study presents a comprehensive techno-economic and spatial assessment aimed at determining the most suitable areas for large-scale green hydrogen production in Luderitz, Namibia. The analysis employs the Analytical Hierarchy Process integrated with Geographic Information System techniques to evaluate and spatially prioritize potential sites. Critical criteria, including solar irradiance, wind velocity, land use, and proximity to essential infrastructure, were systematically weighted and overlaid to generate suitability classifications. The results indicate that approximately 20% of the study area exhibits high suitability, 68% moderate suitability, 8% marginal suitability, and 4% is unsuitable for the development of integrated wind and solar energy. These findings provide a robust scientific basis for guiding policy formulation, investment planning, and the spatial optimization of Namibia's emerging green hydrogen industry.

Keywords: AHP; green hydrogen; GIS; optimization; solar PV; wind farm

1. Introduction

The global transition toward sustainable and low-carbon energy systems has intensified interest in green hydrogen as a key driver for decarbonizing sectors such as heavy industry, transport, and power generation. Energy and industrial sectors are responsible for 42% and 26% of CO₂ emissions worldwide, respectively [1]. Green hydrogen, which is produced by using renewable energy sources, offers an environmentally friendly alternative to fossil-fuel-based hydrogen, contributing to both energy security and climate change mitigation. However, the feasibility and competitiveness of green hydrogen production are highly dependent on spatial and environmental factors, including renewable energy potential, water availability, infrastructure accessibility, and proximity to demand centers.

Several studies have utilized a combination of GIS and Multi-Criteria Decision-Making (MCDM) techniques to determine the most suitable locations for establishing renewable energy farms. Kamati et al. [2] used AHP and GIS approach to determine potential locations for wind and solar photovoltaic (PV) energy plants in the Central and North regions of Namibia. Their findings showed that the highest potential for solar PV energy plants is in the northwest, southwest, and southern regions, whereas only the northwest region is highly suitable for wind power plants. Dahani et al [1] also used MCDM and GIS to identify the most promising locations in Morocco for a green ammonia unit through a land suitability analysis. Their findings showed that the levelized cost of ammonia (LCOA) ranges from \$ 646 to \$ 687 per ton. Sun et al [3] presents a framework to evaluate the suitable location and technical potentials for large-scale solar PV and concentrated solar power (CSP) plants by combining GIS and MCDM methods.

Xu et al [4] combined Interval AHP and GIS to select the best wind farm sites in the Wafangdian region, China. Their study employed a multi-criteria decision-making framework to identify feasible areas for wind farm development, emphasizing biodiversity conservation and production safety as primary factors. The study determined the relative importance of evaluation criteria such as social impact, economic benefit, terrain, and eco-environmental protection. The results revealed that 30.2% of the study area was suitable for wind power installation, with only 3.36% classified as highly suitable.

Noorollahi et al. [5] applied geographic information system to determine the potential of wind energy in Markazi province in western Iran. The MCDM method and site selection criterion for wind resources assessment are developed for the study area. Criteria investigated included technical, environmental, economic, and geographic standards. Their results were favorable for electricity production in accordance with international standards from wind in western Iran. The results showed that 28% of the study area has the capacity for installing large wind farms.

Despite Namibia's abundant renewable energy potential and growing national interest in hydrogen development, there is limited detailed research on where green hydrogen production would be most suitable and sustainable. Current feasibility studies often focus on technical and economic factors without considering the full range of spatial, environmental, and infrastructural constraints that impact project viability and suitability. In Lüderitz, challenges such as limited freshwater resources, sensitive coastal ecosystems, and the need for grid and port infrastructure demand careful spatial analysis. Without a systematic GIS-based decision-making framework, site selection for green hydrogen projects risks overlooking key sustainability criteria, potentially leading to a suboptimal or environmentally harmful development.

It is on this basis that study is proposing an AHP methods to evaluate the spatial suitability of Lüderitz, Namibia, for green hydrogen production by weighing key criteria, including renewable energy potential, water resource availability, land use, topography, and proximity to infrastructure. By applying pairwise comparisons to these factors, the AHP method transforms expert judgment into quantitative weights that represent the relative importance of each site selection driver. These weights are then integrated with spatial datasets within a GIS environment to produce a suitability map, providing a multi-criteria decision-making framework for identifying the most favorable areas for hydrogen infrastructure development

2. Materials and Methods

This paper employs a GIS-based multi-criteria decision-making approach to assess the suitability of Lüderitz for green hydrogen production

The methodology employed to identify the optimal sites at Lüderitz has three macro phases of analysis. The first phase of the analysis is screening and data preparation. The primary objective of this phase of analysis is to eliminate the unsuitable areas for further consideration. The second phase of the analysis is to identify a suitable site and define decision criteria for the best site selection. The third phase of the analysis is the use of the AHP to weigh the criteria and identify the best site for wind and solar power plants for green hydrogen production. The evaluation criteria considered in the analysis are climatology (technical), topography, and proximity to infrastructure (economic), as shown in Figure 1.

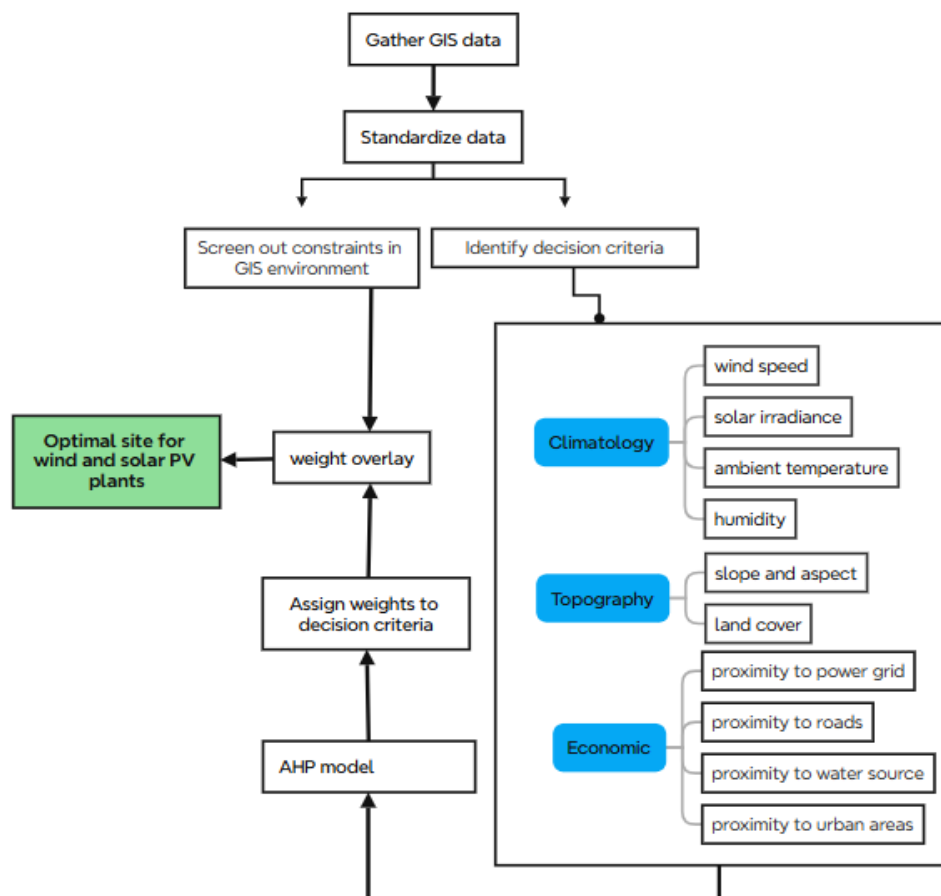


Figure 1. Methodological framework for RE plants site selection.

2.1. Description of the Study Area

Lüderitz is located at 26.6420° S, 15.1639° E, with a total surface area of 112.9 km², excluding the buffer area under exploration. Lüderitz experiences good wind speeds and solar irradiation and is regarded as one of the best areas for hybrid RES plants. The study area is located in the Karas region of the Namib Desert, making it particularly suitable due to its sparse vegetation. Figure 2 shows the map of the study area

The selection of the site is due to the fact that it exhibits best complementary status of wind and solar resources and is also being considered for first Namibian industrial-scale hydrogen production facility.

In this study, ArcGIS 10.8 was utilized to analyze geographic and meteorological data, identifying optimal locations for solar panels and wind turbines that considered factors such as sunlight exposure, wind patterns, topography, and proximity to existing infrastructure. It is used to create detailed maps and models to visualize potential energy yields and assess environmental impacts.

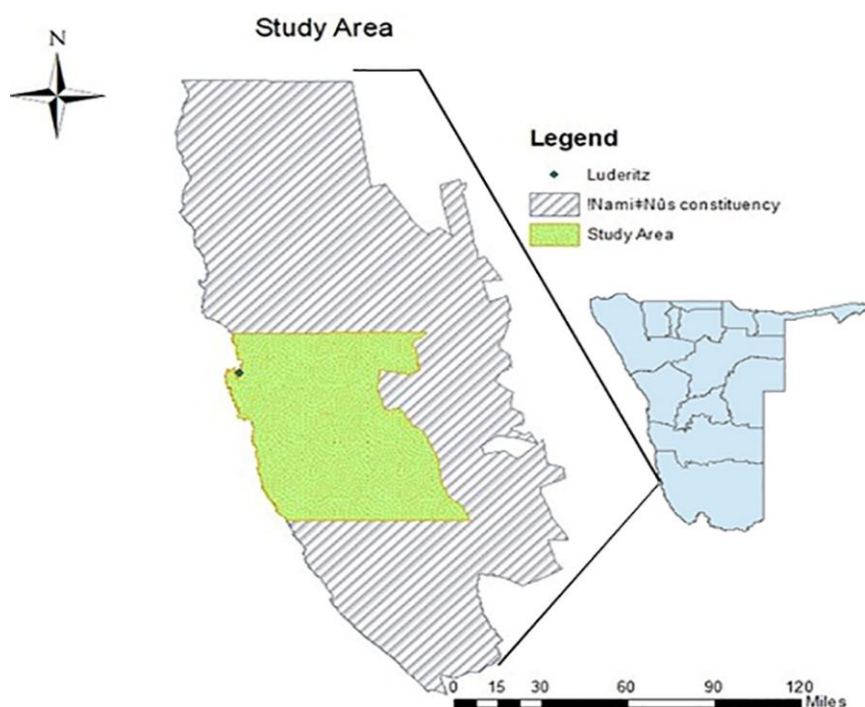


Figure 2. Study area at Lüderitz.

2.2. Identification of Study Area Criteria

Factors that aid in selecting the best site are classified as weighted criteria, while the factors hindering the best site selection are classified as constraints. The weighted criteria influencing location selection are categorized into climatology, topography, and economics. Each criterion is broken down into sub-criteria, with a total of nine criteria considered in this study. These criteria are thoroughly analysed for their characteristics, benefits, and implications in developing of wind and solar PV power plants.

It's important to note that some criteria may be based on energy policies, preferred technologies, site characteristics, and specific country requirements. However, the goal is to obtain an optimum selection of a set of criteria that would enable a renewable energy scheme to perform at its optimum capacity. Criteria such as topography, wind speed, air temperature, road access, power grid access, and solar irradiation are the weighted criteria and are to be incorporated into the Analytic Hierarchy Process MCDM approach

2.3. Input Data

Meteorological data, essential for assessing energy potential, can lead to erroneous conclusions if influenced by calibration errors or equipment malfunctions in weather stations or satellites. Therefore, the data collected in this study were investigated for these potential errors, ensuring data accuracy through validation and cross-verification. This study utilized a dual-source validation approach, comparing meteorological data from the Global Wind and Solar Atlases against NASA Earthdata. The investigation focused on verifying wind speeds, solar irradiance, and ambient temperatures. The study utilized standard deviation to detect anomalous data points and noise, ensuring that sudden, non-physical fluctuations did not negatively affect the energy potential assessments. This comparative synthesis allowed for the removal of outliers, resulting in a high-fidelity dataset suitable for reliable energy modeling. The data used in this study were obtained from different spatial references, including related literature, open sources, and government agencies, as shown in **Table 1** **Error! Reference source not found.** All partial data were converted to the projected UTM-WGS84 coordinate system for accuracy purposes. Using the imagery view in ArcGIS, some vectors were constructed.

An overview of the threshold criteria for constraint factors influencing the suitability of an area for both wind and solar power plant development is provided in Table 2.

Table 1. Description of spatial datasets, formats, and data sources used in the green hydrogen site-suitability analysis.

Data collected	Data type	XY Coordinate system	Data source
Wind speed at 100m	Raster file	WGS 1984_UTM_Zone_33S	Global Wind Atlas
Solar irradiation	Raster file	WGS 1984_UTM_Zone_33S	Global Wind Atlas
Ambient Temperature	Raster file	WGS 1984_UTM_Zone_33S	Global Solar Atlas
Humidity	Raster file	WGS 1984_UTM_Zone_33S	NASA
Slope	Vector (shapefile)	WGS 1984_UTM_Zone_33S	Open Topography
Distance from water bodies (Sea)	Vector file	WGS 1984_UTM_Zone_33S	Constructed
Important Bird Areas	Vector (Shapefile)	WGS 1984_UTM_Zone_33S	BirdLife International
Land cover	Vector (shapefile)	WGS 1984_UTM_Zone_33S	Esri Land cover in collaboration with Livingatlas.
Airports	Vector (shapefile)	WGS 1984_UTM_Zone_33S	Constructed
Roads	Vector (shapefile)	WGS 1984_UTM_Zone_33S	The World Bank
Power lines	Vector (shapefile)	WGS 1984_UTM_Zone_33S	NamPower
Urban Area	Vector (shapefile)	WGS 1984_UTM_Zone_33S	Constructed

Table 2. Constraints analysed for installing solar PV, wind power plants, and green hydrogen production facilities.

Constrain	Buffer zone (meters)	Suitability	Reference
Protected Areas	≤ 500	Not Suitable	[6]
	> 500	Suitable	
Urban areas	≤ 500	Not Suitable	[7]
	> 500	Suitable	
Important Bird Areas	≤ 1 000	Not Suitable	[8]
	> 1 000	Suitable	
International and Military Airports	≤ 25 000	Not Suitable	[9]
	> 25 000	Suitable	

Domestic Airports	$\leq 2\,500$	Not Suitable	[9]
	$> 2\,500$	Suitable	
Forests (Land cover)	≤ 100	Not Suitable	[10]
	> 100	Suitable	

2.4. Screening Out Constraints

Constraints include mostly environmental regulations related to airports, noise control, forests, agricultural lands, protected areas (including wetlands, national parks, important bird areas, and water bodies). These areas, including their buffer zones, must be excluded from further consideration of green hydrogen suitability assessments.

2.4.1. Existing Airports

Wind farm development near airports is restricted due to collision risks, radar/navigation interference, wake turbulence, and impacts on future development. A 25,000 m buffer zone is required for international/military airports, and 2,500 m for smaller airfields [9]. Since Lüderitz Airport is a small domestic airfield, a 2,500 m buffer was applied to the wind and solar site selection area and removed.

2.4.2. Urban Areas

Setting up a wind farm in urban areas involves several considerations to maximize efficiency, minimize impacts, and comply with regulations. 500 m from urban areas is stated to be the minimum threshold distance to set up a wind farm. Placing wind farms away from urban areas helps minimize the impact of noise and visual pollution on the local population.

While rare, there is a risk of mechanical failures, such as blade throw or ice throw, where parts of the turbine or ice accumulated on blades can be projected at high speeds. Keeping wind farms away from populated areas mitigates these safety risks.

2.4.3. Protected Area

Protected areas such as natural, archaeological, and historic sites, tourist areas, wildlife, and areas of cultural heritage were studied. Such protected areas and areas within a 500m buffer zone from such areas are classified as unsuitable areas.

2.4.4. Land Cover

Certain types of land, including forests, woodlands, and wetlands, are not suitable for both solar and wind farms. Trees in forests and woodlands hinder wind flow, reducing the efficiency of wind turbines. Wetlands are not conducive to electrical installations due to their unstable and often waterlogged ground conditions. As a result, these areas are excluded from wind farm suitability assessments to ensure optimal performance and safety of the installations. The area under study is located in the Namib desert, with no vegetation longer than one meter covering the land, hence making land cover of very little consideration.

2.4.5. Important Bird Areas

Wind energy can negatively affect birds through collision, deaths, displacement, barriers, and habitat loss or degradation. Therefore, avoiding wind farms on Important Bird Areas (IBA) is the most effective way to prevent or reduce these impacts

2.5. Analytic Hierarchy Process (AHP)

AHP is a structured technique for organizing and analyzing complex decisions, based on mathematics and psychology. It was developed by Thomas L. Saaty in the 1970s, and in 1983, Saaty partnered with Ernest Forman to develop expert software [11]. It represents an accurate approach to quantifying the weights of decision criteria. Individual experts' experiences are utilized to estimate the relative magnitudes of factors through pair-wise comparisons [12]. Each of the respondents compares the relative importance of each pair of items using a specially designed questionnaire. The relative importance of the criteria can be determined with the help of the AHP by comparing the criteria and, if applicable, the sub-criteria in pairs by experts or decision-makers. AHP is one of the most favored and commonly utilized methods in the literature for determining the best locations for installing wind and solar PV energy plants. It is the most widely used multi-criteria decision-making technique integrated within GIS, which assigns weights to criteria and can manage inconsistent judgments.

2.5.1. AHP Mathematical Model

In this study, the following steps are used for identifying optimal sites for RE plant deployment using the AHP technique. First, the decision problem is structured into a hierarchy in the AHP process by defining the main goal (selecting the best locations for RE plants) and the criteria. As shown in Figure 3, the decision problem is organized into a hierarchical model, with the top level representing the objective of selecting the optimal sites for PV utility-scale plants. The second level lists the decision criteria and sub-criteria for wind and solar site selection.

The second step is to compare the criteria using Saaty's numerical scale from one to nine, based on their importance as shown in Table 3. The score points of the criteria are then applied in the construction of a pairwise comparison matrix [11].

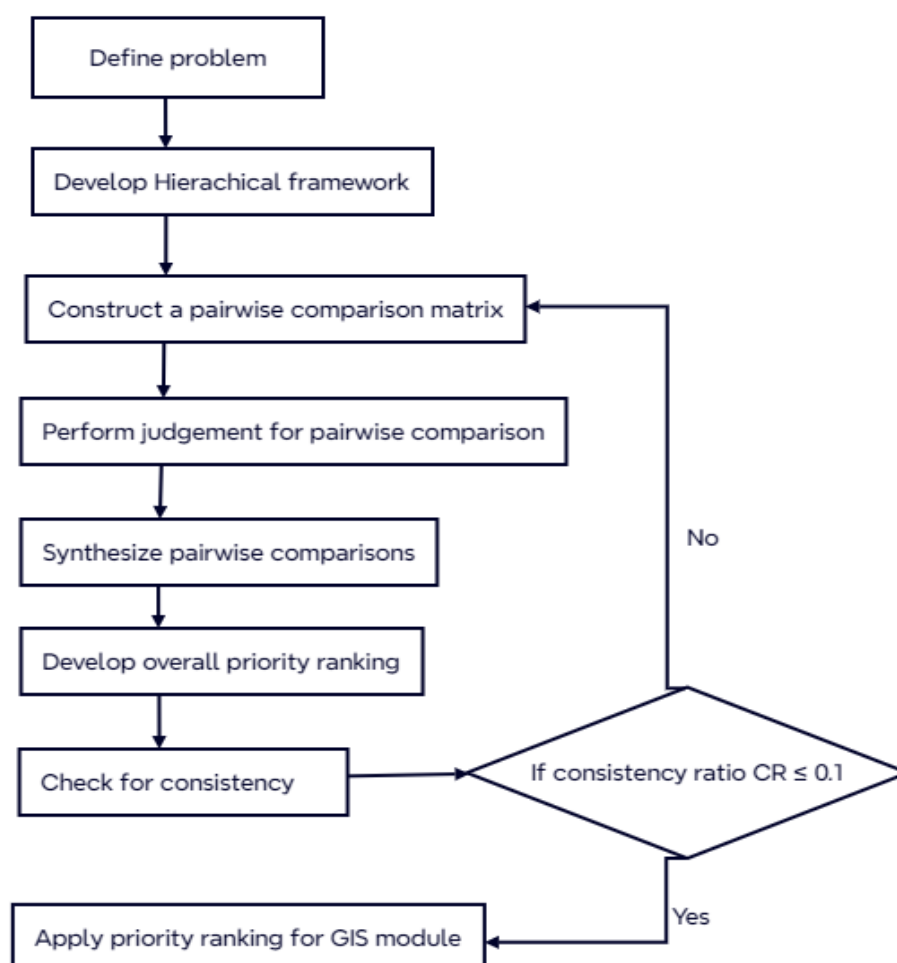


Figure 3. The implemented AHP flowchart.

In this study, the following steps are used for identifying optimal sites for RE plant deployment using the AHP technique; First, the decision problem is structured into a hierarchy in the AHP process by defining the main goal (selecting the best locations for RE plants) and the criteria. As shown in Figure 3, the decision problem is organized into a hierarchical model, with the top level representing the objective of selecting the optimal sites for PV utility-scale plants. The second level lists the decision criteria and sub-criteria for wind and solar site selection, this is followed by comparing the criteria using Saaty's numerical scale from one to nine, based on their importance as shown in Table 3. The score points of the criteria are then applied in the construction of a pairwise comparison matrix [11].

Table 3. Saaty's nine-point scale of relative importance.

Relative importance of criterion x to criterion y	Definition	Explanation.
1	Equal importance	Two criteria contribute equally to the objectives
3	Moderate importance	Experience and judgment slightly favor one criterion over another.
5	Strong importance	Experience and judgment strongly favor one criterion over another.
7	Very strong importance	Experience and judgment very strongly favor one criterion over another.
9	Extreme importance	The evidence favoring one criterion over another is the highest possible order of affirmation
2,4,6, and 8	Intermediate importance between two adjacent judgments	Used for criteria that are very close in importance.

The pairwise comparison matrix C is the square matrix ($n \times n$), where n is the number of criteria. For each cell c_{jk} the matrix C represents the comparison values between the j^{th} row criteria relative to the k^{th} column criterion. If the cell $c_{jk} > 1$, the j^{th} criteria are more important than the k^{th} criteria and vice versa.

$$C = \begin{bmatrix} c_{11} & \cdots & c_{1n} \\ \vdots & \ddots & \vdots \\ c_{n1} & \cdots & c_{nn} \end{bmatrix} \quad (1)$$

Step three involves deriving the normalized pairwise comparison matrix to determine the priority (weights) of each criterion. In a normalized pairwise comparison matrix M , the sum of each column must equal 1. This is achieved by calculating S_{jk} for each cell in matrix C using Equation 2.

$$S_{jk} = \frac{C_{jk}}{\sum_{j=1}^n C_{jk}} \quad (2)$$

Step four is to determine the overall weight vector. The criteria weight vector (W_j) is calculated by averaging across rows to obtain the relative weights as given by equation 3.

$$W_j = \frac{\sum_{j=1}^n S_{jk}}{a} \quad (3)$$

where: a is the number of values in the row.

Step five is to compute the Matrix's consistency ratio (CR). The degree of consistency in the analysis is considered acceptable if the $CR \leq 0.1$; otherwise, the judgments must be revised to identify and correct the source of the inconsistency. CR and CI are calculated using equations 4 and 5, respectively.

$$CR = \frac{CI}{RI} \quad (4)$$

$$CI = \frac{\lambda_{\max} - n}{n - 1} \quad (5)$$

where λ_{\max} is the maximum eigenvalue of the comparison matrix, and n is the size of the matrix. RI represents values of the random consistency index depending on the number of criteria N considered in matrix C. Saaty's RI values are shown in Table 4.

Table 4. Saaty's random consistency index [11].

N	1	2	3	4	5	6	7	8	9	10	11	12	13
RI	0	0	0.58	0.9	1.12	1.24	1.32	1.41	1.45	1.49	1.51	48	1.56

2.6. Solar Power Analysis

Criteria affecting the site selection of a solar power plant are analyzed in this section. All sub-criteria are classified according to their suitability. The criteria and their classification ranges are shown in **Table 5** **Error! Reference source not found..**

Table 5. Criteria influencing the Optimal site selection for a Solar Power Plant.

Criteria	Sub-criteria	Classes	Suitability	Class Rating	Reference
Climatology	Solar irradiation in (kWh/m ² /year)	>2 263	Highly suitable	4	[2]
		2 153.5 – 2 263	Moderately Suitable	3	
		1 953.36 – 2 153.5	Barely suitable	2	
		<1 953.36	Unsuitable	1	
	Air temperature in °C	14.70 – 17	Highly suitable	4	[2]
		17 - 20	Moderately Suitable	3	
		20 – 24.10	Barely suitable	2	
		>24.10	Unsuitable	1	
	Humidity (%)	<65.40	Highly suitable	4	[12]
		65.40 -73.50	Moderately Suitable	3	
		73.50 – 91.70	Barely suitable	2	
		91.70	Unsuitable	1	
Topography	Slope (%)	<3%	Highly suitable	4	[13]

		3-7%	Moderately Suitable	3	
		7-10%	Barely suitable	2	
		>10%	Unsuitable	1	
	Aspect (°)	0 - 22.5 and 337.5 - 360	Highly suitable	4	[14]
		22.5 - 67.5 and 292.5 337.5	Moderately Suitable	3	
		67.5 - 90 and 270 - 292.5	Barely suitable	2	
		90 - 270	Unsuitable	1	
Economics	Proximity to sea in meters	< 10 000	Highly preferred	4	
		1000 - 20 000	Moderately preferred	3	
		20 000 - 30 000	Barely preferred	2	
		>30 000	Least preferred	1	
	Proximity to road infrastructures in meters	100 - 5 000	Highly preferred	4	[2,13]
		5 000 - 10 000	Moderately preferred	3	
		10 000 - 20 000	Barely preferred	2	
		>20 000	Least preferred	1	
	Proximity to power line infrastructures in meters	< 5000	Highly preferred	4	[15]
		5000 - 10000	Moderately preferred	3	
		10000 - 20000	Barely preferred	2	
		>20000	Least preferred	1	

2.6.1. Solar Irradiation

Solar irradiation is a crucial factor in assessing the potential of a specific region. It measures the amount of energy received per unit area on the Earth's surface, expressed in watt-hours per square meter. PV systems utilize Global Horizontal Irradiation (GHI), which represents the total radiation received by a horizontal surface from above. While solar irradiation is a question of technical feasibility, it's also an economic consideration. For cost-effective operations, solar PV panels require a minimum GHI of 1300 kWh/m²/y [2]. Raster format Global Horizontal Irradiation data was collected from the Global Solar Atlas at 250 m for GIS analysis. It represents yearly time average from 2013 to 2023 (10 years) in kWh/m². Figure 4(a) shows the unclassified and re-classified ranges of daily average solar irradiation in kWh/m². The 4 suitability classes are shown in Figure 4(b).

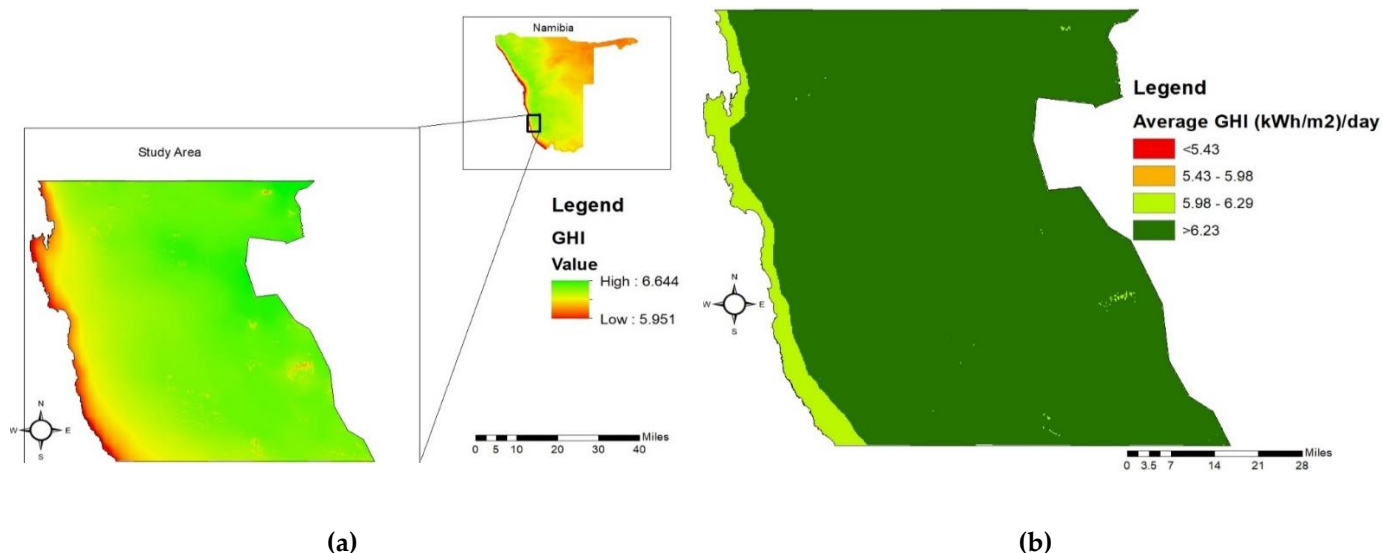


Figure 4. Daily average solar irradiation (a) Unclassified and (b) Reclassified map.

2.6.2. Air Temperature

An increase in air temperature decreases panel efficiency. Kocabaldir and Yucel [12], have shown that the amount of generated energy declines by about 0.4%-0.5% for every 1°C rise in the cell temperature at temperatures above 25 °C. Solar efficiency and temperature relationship is given by equation 6. Their relationship can be described by a linear equation.

$$\eta(T) = \eta_{ref}[1 - \beta(T - T_{ref})] \quad (6)$$

where:

- $\eta(T)$ is the efficiency of the PV cell at temperature T.
- η_{ref} is the reference efficiency of the PV cell at the reference temperature (usually 25°C or 298 K).
- T is the operating temperature of the PV cell.
- T_{ref} is the reference temperature, typically 25°C (298 K).

2.6.3. Air Temperature

An increase in air temperature decreases panel efficiency. Kocabaldir and Yucel [12], have shown that the amount of generated energy declines by about 0.4%-0.5% for every 1°C rise in the cell temperature at temperatures above 25 °C. Solar efficiency and temperature relationship is given by equation 6. Their relationship can be described by a linear equation.

$$\eta(T) = \eta_{ref}[1 - \beta(T - T_{ref})] \quad (7)$$

where:

- $\eta(T)$ is the efficiency of the PV cell at temperature T.
- η_{ref} is the reference efficiency of the PV cell at the reference temperature (usually 25°C or 298 K).
- T is the operating temperature of the PV cell.
- T_{ref} is the reference temperature, typically 25°C (298 K).
- β is the temperature coefficient of efficiency, which is a negative value representing the rate of efficiency decrease per degree Celsius increase in temperature. It is typically provided by the manufacturer and might be in the range of -0.2%/°C to -0.5%/°C for many silicon-based PV cells.

The solar cell temperature can be calculated from equation 7.

$$T_c = T_a + \left(\frac{T_{ref} - 20^\circ\text{C}}{800} \right) \times \text{Irradiance} \quad (8)$$

where T_c is the solar cell temperature

T_a is the air temperature and

T_{ref} is the nominal reference temperature.

Therefore, areas with lower temperatures have increased solar efficiency, making them preferred for solar installations. The unclassified and reclassified map for temperature averages is shown in Figure 5. From the map, cooler temperatures can be observed along the coast and get warmer as you go inland. The lowest average temperature recorded is 15.4 °C to 20.9 °C, placing the overall study area in the high and moderate suitable classes as shown in Figure 5.

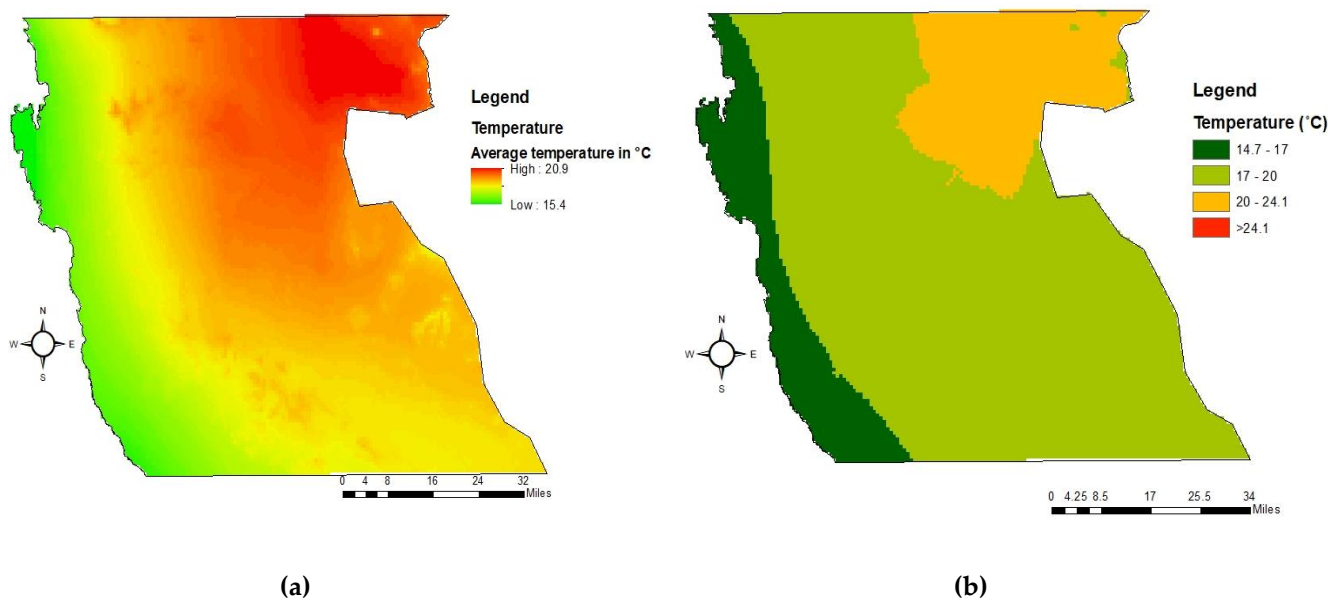


Figure 5. The average temperature map (a) unclassified and (b) reclassified.

2.6.4. Humidity

Humidity can affect solar efficiency in two ways. Tiny water droplets, or water vapor, can collect on solar panels and reflect or refract sunlight away from solar cells. This reduces the amount of sunlight reaching them and, consequently, their ability to produce electricity. In addition, consistent hot, humid weather can degrade the solar panels over their operational lifespan. This mostly applies to both crystalline silicon cells and thin-film modules. The humidity map generated using data from 2012 to 2022 (obtained at 2 meters) is given in Figure 6.

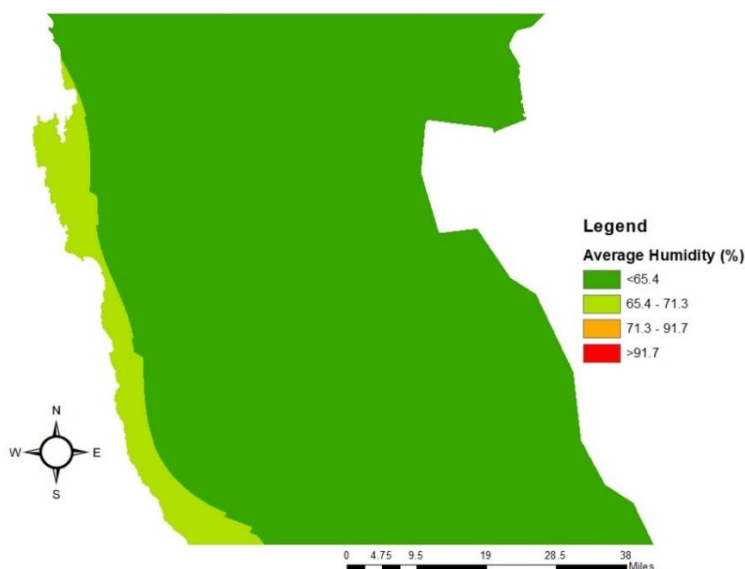
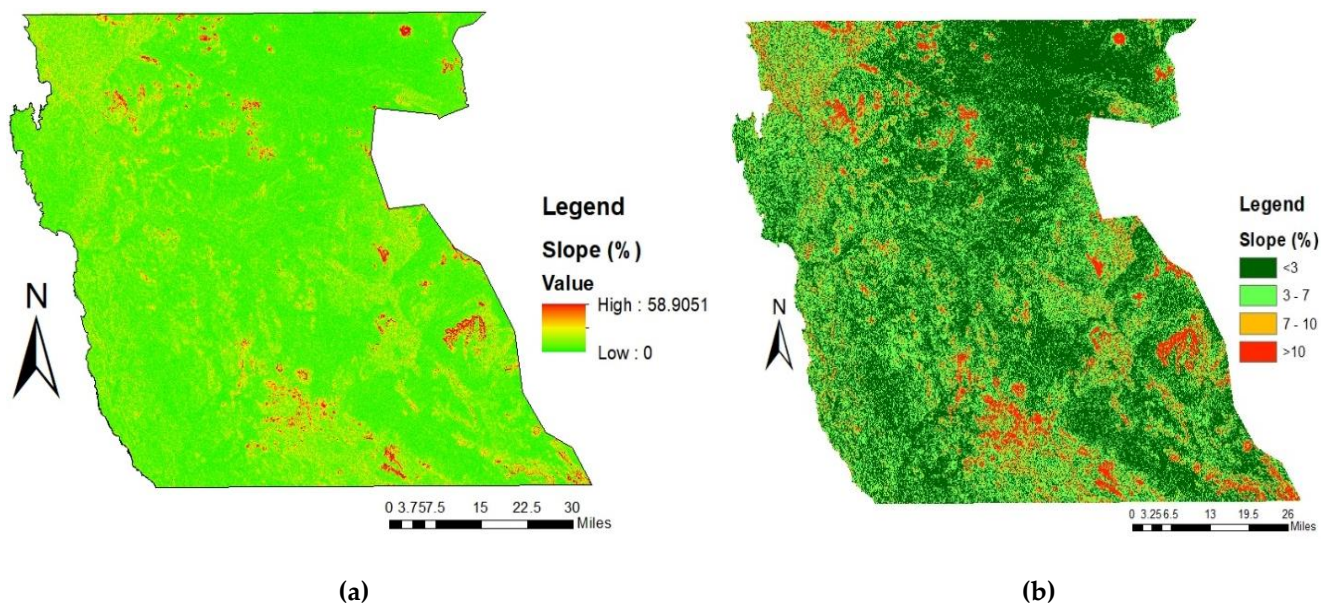


Figure 6. Average relative humidity.

2.6.5. Slope

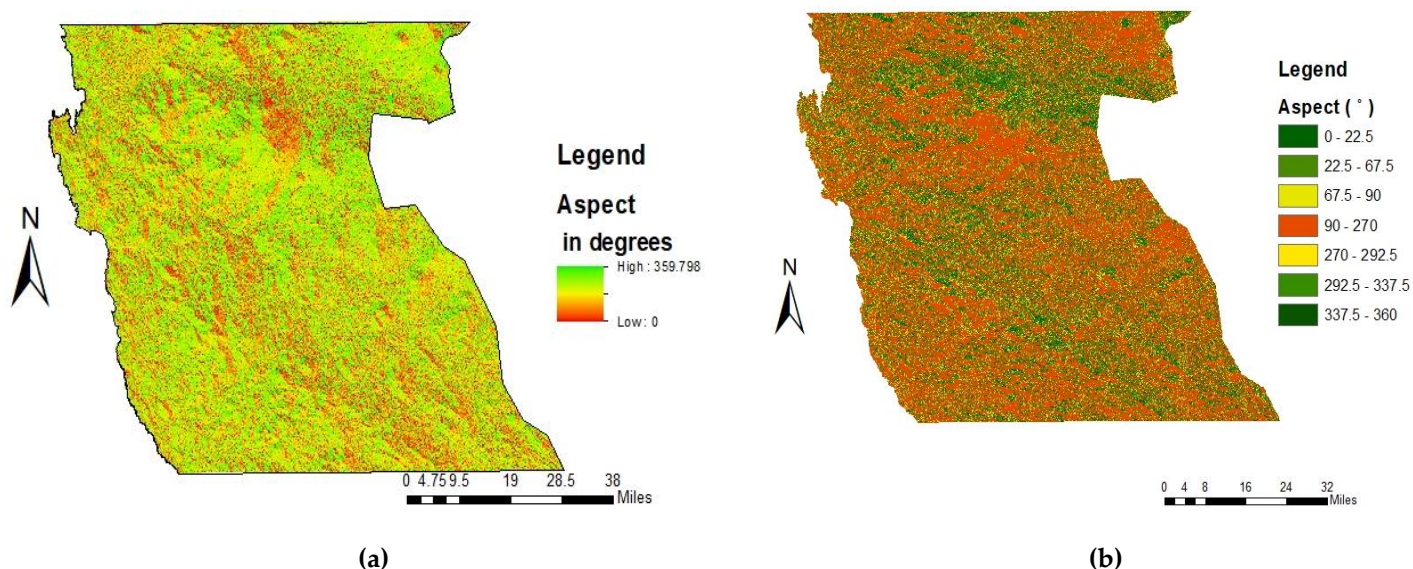
Flat terrain is desired for solar plants. In most studies, only 3%-10% slope degrees have been considered to exclude the very steep areas [7]. As the slope value of 3% increases, the cost of investment increases gradually.

From the slope map above, more than 90% of the total study area has good slopes. Hence, making it very suitable for solar installations. The slope orientation map is shown in Figure 7.

**Figure 7.** Map of slopes (a) unclassified and (b) reclassified.

2.6.6. Aspect

In this criterion, north-facing lands are preferred because south-facing lands have low suitability. This is due to the sun moving across the sky from east to west in Namibia, with the highest point directly north at noon. When solar panels face north, they capture sunlight throughout the day, maximizing their power output. The aspect mapping of the study area is shown in Figure 8.

**Figure 8.** Aspect orientation (a) Unclassified and (b) classified map.

2.6.7. Proximity to Sea

Due to the renewable resources assessment in this study being carried out for green hydrogen, proximity to the sea is of vital consideration. This is to optimize the distance between the renewable energy plants, the electrolysis plant, the desalination and the water source(sea). The proximity to the sea analysis is shown in the map shown as **Figure 9****Error! Reference source not found.**

Figure 9. Classified distance from the sea.

A green hydrogen plant should be situated at an optimum distance from the sea to facilitate a shorter distance to water desalination. When renewable power plants are placed close to the sea, it minimizes the power losses in transmission over long distances to desalination and electrolysis plant. Hence, locating the plant at an optimal distance from the sea is essential for operational efficiency, cost-effectiveness, and environmental sustainability.

Additionally, a green hydrogen plant needs to be in optimum proximity to the sea because the pipes carrying produced hydrogen to the seaports need to be short. This is to reduce the cost of pipes and to reduce the exposure of hydrogen to more environmental conditions with an increase in pipe length.

2.6.8. Proximity to Roads

Transportation cost is a dominant factor for any power plant installation. This is the case for hydrogen production plants, where hydrogen could be transported using multi-element gas container trailers, etc. Thus, the areas far from roads are not economically feasible and less suitable. Therefore, in this study, locations with less than 5000 meters distance are selected as highly suitable sites for solar PV. Locations with 5,000 meters to 10,000 meters are suitable, 1 0000 meters to 20,000 meters are moderately suitable, and greater than 20,000 meters are considered unsuitable (see **Figure 10****Error! Reference source not found.**).

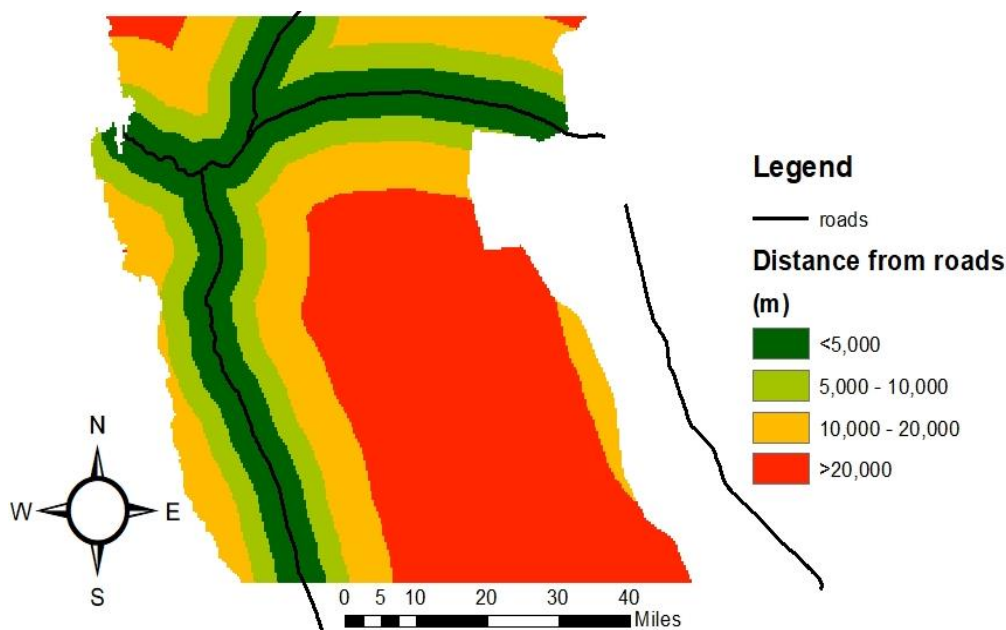


Figure 10. Road Distribution Map.

2.6.9. Proximity to Power Lines

For this study, the connection to the power line is solely to feed extra energy into the grid, not to draw energy from it. All renewable plants proposed in this study are utility-scale plants that can either connect directly to substations or tapping a transmission line of 69 kV or higher. Figure 11 shows proximity analysis for power transmission lines.

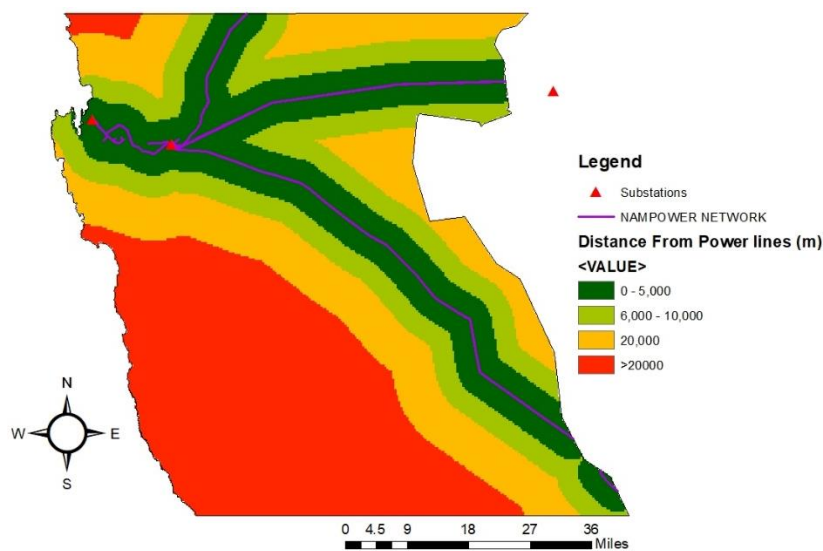


Figure 11. Power lines distribution Map.

2.7. Wind Power Analysis

This section analyzes site selection criteria for wind power plants. Economic criteria, common to both solar and wind, were discussed previously. Wind farm site selection criteria are classified into Table 6 according to their suitability ranges.

Table 6. Criteria influencing the Optimal site selection for a Wind Power Plant.

Criteria	Sub-criteria	classes	suitability	Rank	reference
----------	--------------	---------	-------------	------	-----------



Climatology	Wind speed	>9.5	Highly suitable	4	[16]
		6.9-9.5	Moderately suitable	3	
		5.6-6.9	Barely suitable	2	
		<5.6	unsuitable	1	
Topography	Slope (%)	0 – 2.9	Highly suitable	4	[2]
		2.9-5.7	Moderately suitable	3	
		5.7 – 8.5	Barely suitable	2	
		>8.5	unsuitable	1	
Economic	Proximity to roads (meters)	100 - 5000	Highly suitable	4	[13][16]
		5000 – 10 000	Moderately suitable	3	
		10 000 - 20 000	Barely suitable	2	
		>20 000	unsuitable	1	
	Proximity to power lines (meters)	250 – 5 000	Highly suitable	4	[15]
		5 000 – 10 000	Moderately suitable	3	
		10 000 – 20 000	Barely suitable	2	
		>20 000	unsuitable	1	
	Distance from the sea	<10 000	Highly suitable	4	
		10 000 – 20 000	Moderately suitable	3	
		20000 – 30 000	Barely suitable	2	
		>30 000	unsuitable	1	

2.7.1. Wind Speed

The wind resource is a very important technical criterion that affects the siting of a wind farm in any location. The amount of wind energy that can be generated from a particular location is proportional to the cube of the wind speed at that location and is given by equation 8:

$$P(v) = \frac{1}{2} \rho A v^3 \quad (9)$$

where:

- $P(v)$ is the average wind energy in watts (W) at a particular location,
- ρ is the air density in kg/m^3 ,
- A is the sweep area in m^2 of the rotor blades,
- v is the average wind speed in m/s

Wind data raster data file was obtained for a period of 10 years (2013 – 2023). **Figure 12Error! Reference source not found.**(a) shows the unclassified wind speed ranges of the study area. Good wind speeds are observed as one moves close to the coastline. The ArcGIS reclassifying tool was applied to wind speed raster data to reclassify it into four suitability classes to find the class each area falls. The reclassified map is shown in **Figure 12Error! Reference source not found.** (b).

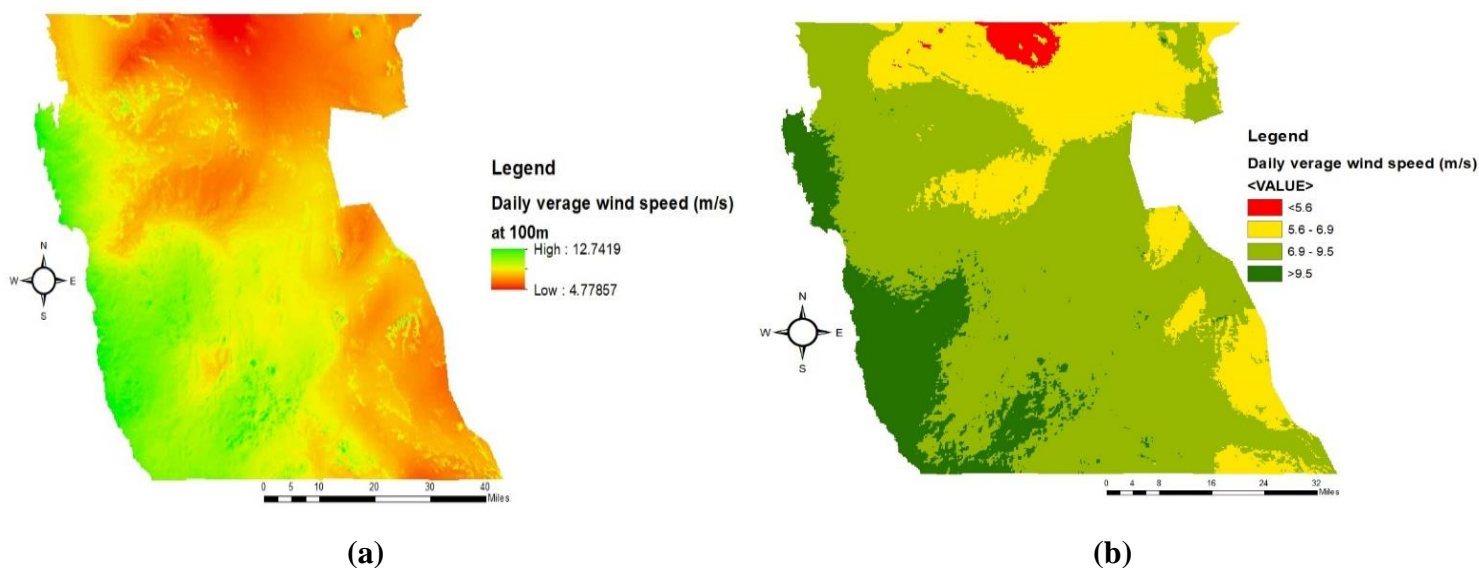


Figure 12. Daily average wind speed at 100-meter height (a) unclassified Map (b) reclassified Map.

2.7.2. Slope

Slope plays a major role in renewable energy installation. It is worth noting that the solar site selection suitability classes for slopes are different from those of wind. The reclassified map of the slope is shown in Figure 13

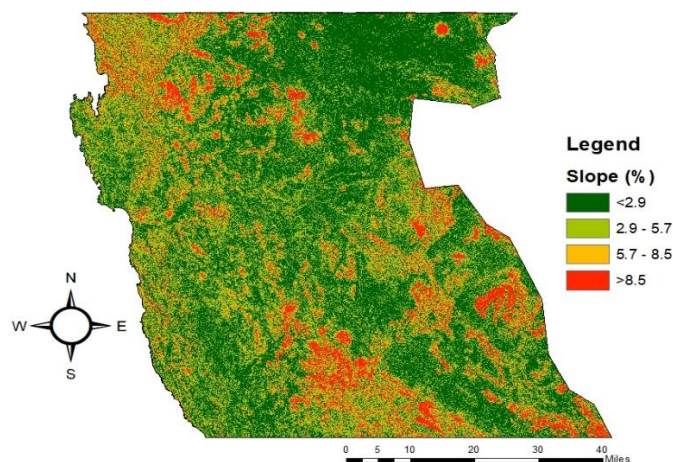


Figure 13. Slope Ratio Distribution Map.

An increase in slope ratio decreases wind speed. When the slope ratio is less than 2.9%, the surface is highly suitable, and greater than 8.5% is said to be unsuitable.

3. Results and Discussion

This section presents the results of the GIS-AHP-based site suitability assessment for green hydrogen production. The results include the relative weights of the selected evaluation criteria derived from the Analytical Hierarchy Process, as well as the spatial distribution of suitability classes generated through GIS-based analysis.

3.1. Constrained Areas Union

The union analysis tool in ArcMap was used to combine all constraint layers into a single layer. In Figure 14, the study area map is divided into suitable (unconstrained) and unsuitable (con

strained) locations for wind and solar plant installations. A total area of 11 344.53km² was considered for the RE analysis. 82.40 km² was found to house constraints, making the remaining area of 11,262.12 km² available for weighted criteria analysis.

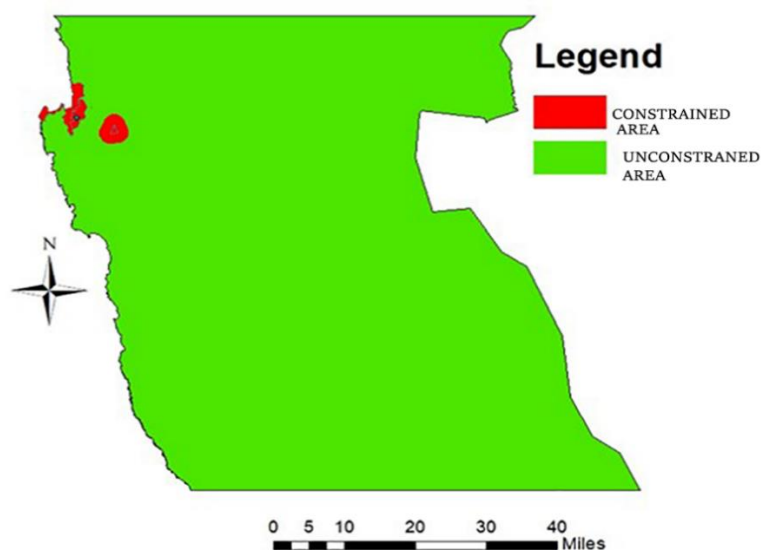


Figure 14. Constrained Areas Union Map.

3.2. Solar PV Pairwise Comparison

The pairwise comparison matrix was generated using Saaty's nine-point scale. Table 7 shows the criteria comparison and the assigned Saaty's degree of importance.

Table 7. The criteria comparison and the assigned Saaty's degree of importance.

		Criteria		More important	scale
i	j	A	B	A or B	1-9
1	2	Solar irradiation	Temperature	A	5
1	3		Slope	A	8
1	4		Aspect	A	8
1	5		Humidity	A	8
1	6		Distance from sea	A	4
1	7		Distance from powerlines	A	6
1	8		Distance from roads	A	6
2	3		Temperature	Slope	A
2	4	Aspect		A	7
2	5	Humidity		A	5
2	6	Distance from sea		A	2
2	7	Distance from powerlines		A	2
2	8	Distance from roads		A	2
3	4	Slope	Aspect	A	2
3	5		Humidity	A	2
3	6		Distance from sea	B	7
3	7		Distance from powerlines	B	4

3	8		Distance from roads	B	4
4	5	Aspect	Humidity	A	1
4	6		Distance from sea	B	7
4	7		Distance from powerlines	B	6
4	8		Distance from roads	B	6
5	6	Humidity	Distance from sea	B	6
5	7		Distance from powerlines	B	4
5	8		Distance from roads	B	4
6	7	Distance from sea	Distance from powerlines	A	3
6	8		Distance from roads	A	3
7	8	Distance from powerlines	Distance from roads	A	1

Average solar irradiation and average air temperature were found to be the most important as they determine the energy output capacity of solar PV plant as shown in Figure 15. Secondly, proximity to the sea and roads and power line follow in importance as they influence the infrastructure cost. humidity, slope, and aspect are less important as their effect on solar PV output power is minimal although it is of vital importance to consider them.

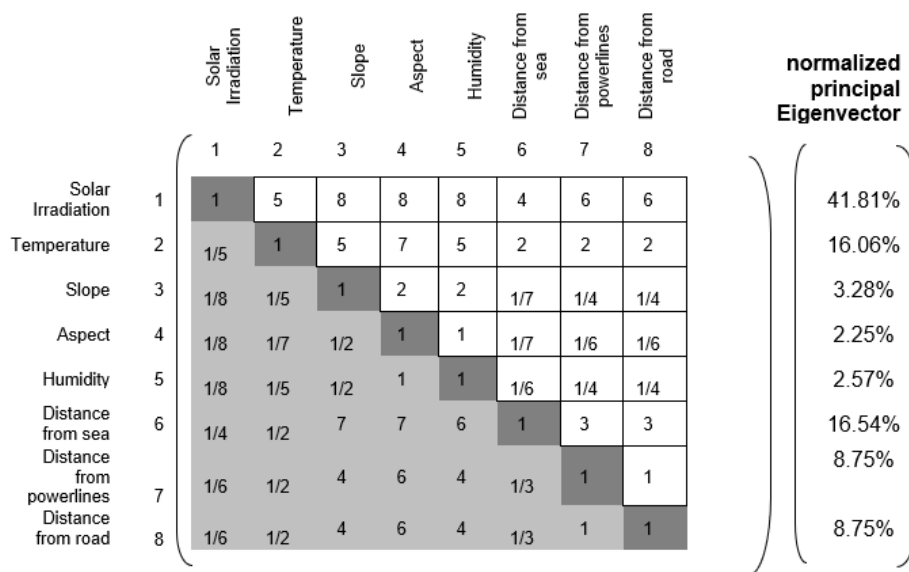


Figure 15. 8 by 8 Pairwise comparison matrix solar site selection.

3.2.1. Computing Weights for Criteria

The weights of solar PV criteria were determined using equation 3 and results are as are given in Table 8. The consistency ratio was calculated using equation 4. The largest eigenvalue (λ) was found to be 8.564 after performing six iterations, and the random consistency index equals 1.41 for 8 criteria. The consistency ratio CR was found to be 0.057 (5.7%), which is acceptable.

Table 8. Criteria Weighs for Solar Photovoltaic Site Evaluation.

Criterion	Weight
1 Solar irradiation	42.1%

2	Temperature	16.0%
3	Slope	3.2%
4	Aspect	2.2%
5	Humidity	2.5%
6	Distance from the sea	16.6%
7	Distance from powerlines	8.7%
8	Distance from roads	8.7%
Eigenvalue		$\lambda_{\max} = 8.564$
Consistency ratio		CR = 0.057

3.2.2. Weight Overlay

The AHP-GIS weight overlay tool in ArcGIS was used to combine all solar criteria to generate the overall suitability map for solar PV site selection. The criteria maps' scales were reclassified to a common scale. The new scale has four classes: Class four is highly suitable, class three is moderately suitable, class two is barely suitable, and class 1 is unsuitable. Weight overlay is given by equation 9.

$$W = \sum_{i=1}^n X_i \times W_i \quad (10)$$

where W is the weighted overlay, n is the number of decision criteria, X_i is the normalized criterion, and W_i is the respective weight of the criterion. The cell/pixel values of the raster layers are multiplied by their weight/percentage influence obtained by AHP analysis, and the results are added together to create the solar PV suitability output raster map shown in **Figure 16**. **Error! Reference source not found.**

The distribution of most suitable sites is predominantly along the western edge areas, particularly along the coastline. Factors such as high solar irradiance and minimal environmental or topographical obstacles make this area ideal for solar projects. Moderately suitable areas extensively cover the central and eastern parts of the region. These areas offer moderate potential for solar installations.

They have excellent solar irradiance and decent land conditions, making them viable options for solar projects (second option). However, they might require more investment or technology to achieve optimal energy production compared to highly suitable areas. Barely, suitable areas are scattered sparsely across the map. These areas are the least favorable for solar energy projects due to likely suboptimal conditions, such as unsuitable slopes and distance from economic aspects.

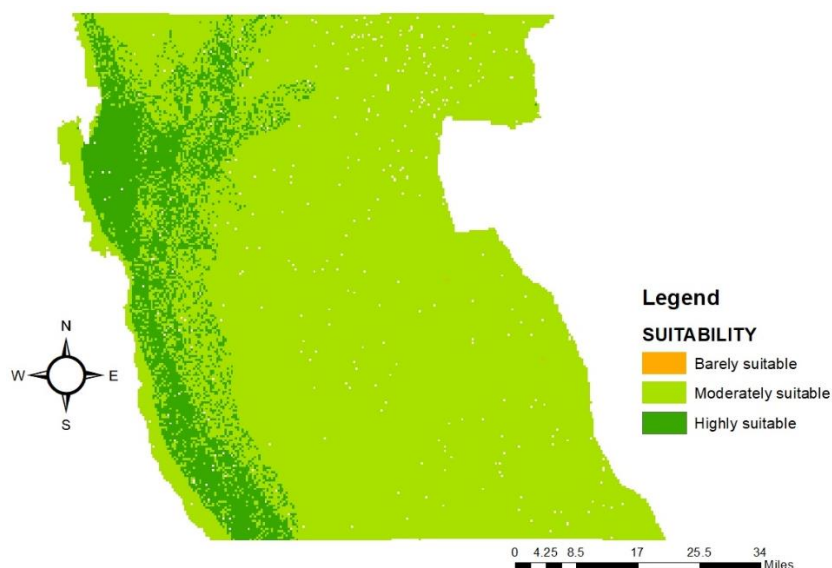


Figure 16. Solar PV suitability map.

3.3. Wind Pairwise Comparison Matrix

The pairwise comparison matrix was generated based on the wind criteria comparison using Saaty's nine-point scale, as shown in Table 9. The assigned Saaty's points were analysed until the matrix was consistent ($\leq 10\%$).

Table 9. Wind criteria comparison and the assigned Saaty's degree of importance.

		Criteria		More important	scale
i	j	A	B	A or B	1-9
1	2	Wind speed	Slope	A	8
1	3		Distance from the sea	A	5
1	4		Distance from powerlines	A	7
1	5		Distance from roads	A	7
2	3	Slope	Distance from the sea	B	6
2	4		Distance from powerlines	B	5
2	5		Distance from roads	B	5
3	4	Distance from the sea	Distance from powerlines	B	3
3	5		Distance from roads	B	3
4	5	Distance from powerlines	Distance from powerlines	A	1

In wind site selection and suitability analysis, wind speed is the most critical criterion, followed by Economic criteria while topography (slope) is considered least significant as presented in Figure 17.

		Wind speed	Slope	Distance from sea	Distance from powerlines	Distance from roads	
		1	2	3	4	5	
Wind speed	1	1	8	5	7	7	normalized principal Eigenvector
Slope	2	1/8	1	1/6	1/5	1/5	
Distance from sea	3	1/5	6	1	3	3	
Distance from powerlines	4	1/7	5	1/3	1	1	
Distance from roads	5	1/7	5	1/3	1	1	
							58.33%
							3.27%
							19.86%
							9.27%
							9.27%

Figure 17. A 5 by 5 pairwise comparison matrix for this Study's wind farm site selection.

3.3.1. Computation of Weights for the Criteria

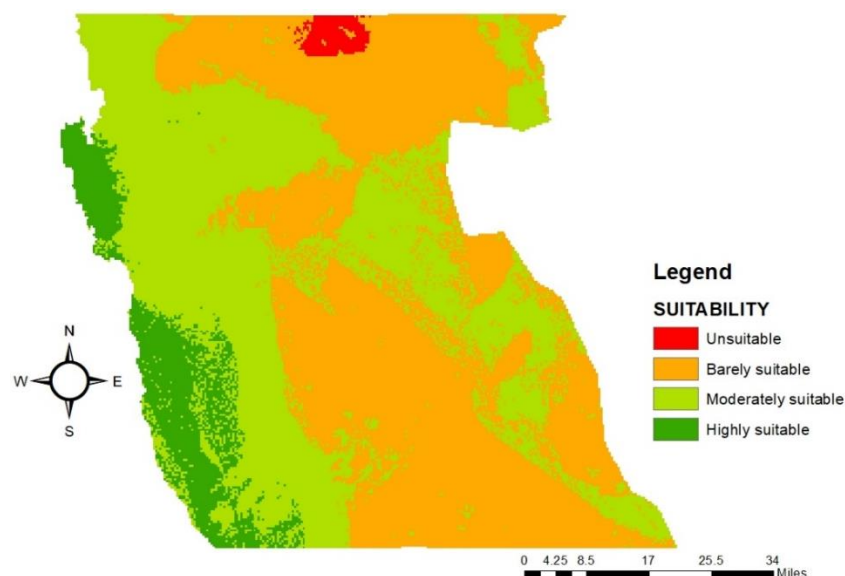
The weights of wind criteria were determined using equation 3 and are as given in Table 10. The consistency ratio was calculated using equation 4. Principal eigenvalue (λ_{\max}) was found to be 5.376 while pairwise matrix was considered consistent only when λ_{\max} is equal to or more than the number of layers examined. The random consistency Index gave 1.12 for 5 criteria. The consistency ratio CR was found to be 0.084 (8.4%), which is said to be acceptable.

Table 10. Calculated weights for wind farm site selection criteria.

Criterion	Weight
1 Wind speed	58.3%
2 Slope	3.3%
3 Distance from the sea	19.9%
4 Distance from powerlines	9.3%
5 Distance from roads	9.3%
Eigenvalue	$\lambda_{\max} = 5.376$
Consistency ratio	CR = 0.084

3.3.2. Weight Overlay

The AHP-GIS weight overlay tool in ArcGIS was utilized to integrate all wind-related criteria and produce an overall wind farm site suitability map. Each criterion map was reclassified onto a unified four-class scale: class four indicating high suitability, class three moderate suitability, class two low suitability, and class one unsuitable. The weighting calculation is detailed in Equation 9. In Figure 18, it is observed that the western part of the study area has extensive areas that are either moderately suitable or highly suitable. The central and eastern regions predominantly show barely suitable areas.

**Figure 18.** Wind farm suitability map.

A small region in the north-central part of the map is marked as unsuitable, making wind farm installation economically and technically unviable. Highly suitable areas found mostly along the coastal line correspond to higher wind speed along the coast and shorter distances to the water source (sea). Unsuitable area corresponds to low wind speeds less than 5.5 m/s and its positions from roads, sea, and power lines.

3.4. Solar-Wind Site Overlay

Solar and wind resource maps were overlaid in ArcGIS, each assigned an equal weight of 50% to reflect their equal significance. The resulting combined optimized map, which also incorporates proximity to infrastructure, is shown in Figure 19. It can be clearly shown that most suitable sites for solar PV and wind farm installations are predominantly located near the coast, highlighting the importance of proximity to the sea as a key criterion in this study. Areas classified as moderately suitable cover over 70% of the study region. Barely suitable zones are primarily found in the northern part.

Wind and solar plants should be situated at an optimum distance from each other to maximize efficiency, energy production, and land use, while addressing operational considerations. These plants leverage complementary resources, as wind and solar energy often balance each other. When solar energy is unavailable, wind energy might still be accessible. Placing these plants at an optimal distance ensures efficient resource utilization and prevents interference. Wind turbines require space to avoid wake effects, and solar panels need unobstructed sunlight. By positioning them correctly, dual land use is possible, maximizing the available area without compromising efficiency.

Additionally, proximity allows for shared infrastructure like roads, transmission lines, and maintenance facilities, reducing overall costs. Proper distancing prevents issues such as solar panel shading by wind turbines and ensures wind turbines do not affect each other's wind flow. Maintenance and monitoring operations become simpler and more cost-effective when plants are closed, allowing for centralized control systems and reduced travel time for maintenance crews.

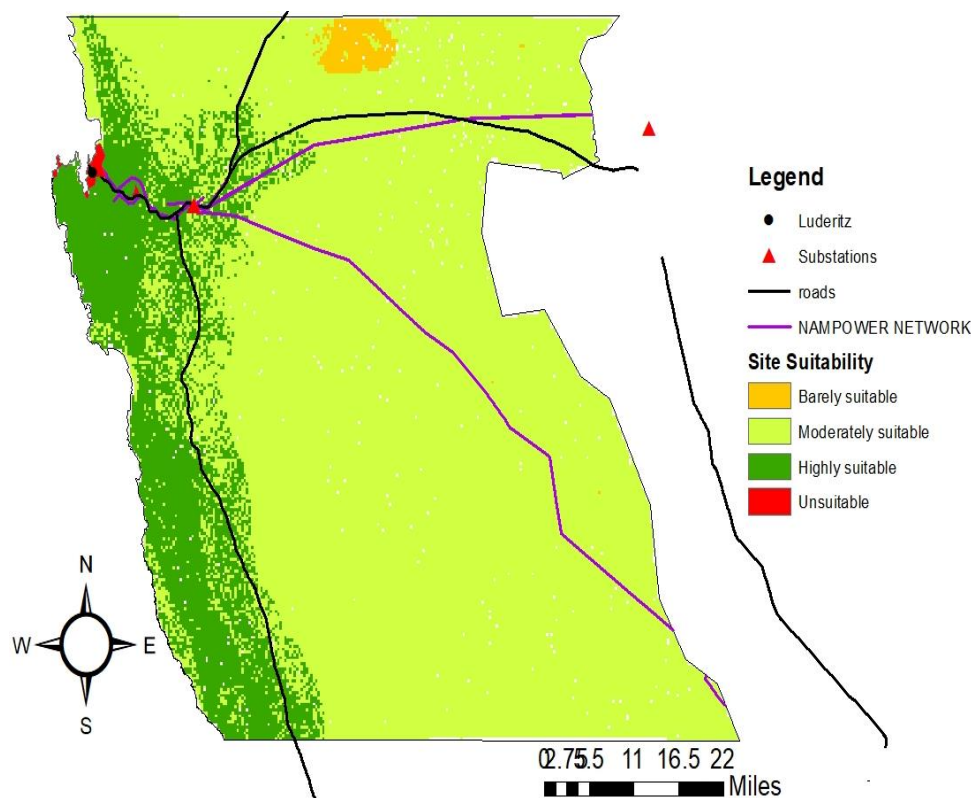


Figure 19. Solar PV and wind energy potential site selection and optimized classes.

4. Conclusion

The integration of AHP and GIS in the analysis of wind and solar site selection has proven to be a highly effective approach. AHP's robust framework for multi-criteria decision-making allowed for a systematic evaluation of all critical criteria, such as wind speed, solar radiation, land use, proximity to infrastructure, and protected areas. By assigning appropriate weights to these criteria through pairwise comparisons, AHP ensures that the most relevant factors are prioritized, resulting in a

comprehensive and objective assessment of potential sites. GIS complements AHP by providing advanced spatial analysis and visualization capabilities. It enabled the integration and management of diverse spatial data layers used in this study, facilitating a holistic analysis of all relevant factors. The spatial analysis tools in GIS apply the weights derived from AHP to generate detailed suitability maps, categorizing areas into distinct classes of suitability. In this research, the analysis of the optimized map revealed that 20% of the area is most suitable, 68% is moderately suitable, 8% is barely suitable, and 4% is unsuitable for wind and solar energy projects.

Overall, the combined use of AHP and GIS in this research has facilitated a thorough and nuanced analysis of potential sites for wind and solar energy projects. This integrated approach ensured the identification of the most viable locations, optimizing economic and technical outcomes by focusing resources on regions with the highest potential. This approach can be applied to other regions for renewable site analysis. This work contributes meaningfully to advancing Namibia's role in the global transition toward sustainable, renewable energy solutions.

References

1. A. Dahani, C. Benqlilou, M. Holz, and C. Scott, "Land Suitability Analysis for Green Ammonia Unit Implementation in Morocco Using the Geographical Information System – Analytic Hierarchy Process Approach," 2024.
2. K. Kamati, J. Smit, and S. Hull, "Multicriteria Decision Method for Siting Wind and Solar Power Plants in Central North Namibia," *Geomatics*, vol. 3, no. 1, pp. 47–68, 2022, doi: 10.3390/geomatics3010002.
3. L. Sun *et al.*, "A GIS-based multi-criteria decision making method for the potential assessment and suitable sites selection of PV and CSP plants," *Resour. Conserv. Recycl.*, vol. 168, p. 105306, May 2021, doi: 10.1016/J.RESCONREC.2020.105306.
4. Y. Xu *et al.*, "Site selection of wind farms using GIS and multi-criteria decision making method in Wafangdian, China," *Energy*, vol. 207, p. 118222, Sep. 2020, doi: 10.1016/J.ENERGY.2020.118222.
5. Y. Noorollahi, H. Yousefi, and M. Mohammadi, "Multi-criteria decision support system for wind farm site selection using GIS," *Sustain. Energy Technol. Assessments*, vol. 13, pp. 38–50, Feb. 2016, doi: 10.1016/J.SETA.2015.11.007.
6. M. Sadeghi and M. Karimi, "GIS-based solar and wind turbine site selection using multi-criteria analysis: Case study Tehran, Iran," *Int. Arch. Photogramm. Remote Sens. Spat. Inf. Sci. - ISPRS Arch.*, vol. 42, no. 4W4, pp. 469–476, Sep. 2017, doi: 10.5194/ISPRS-ARCHIVES-XLII-4-W4-469-2017.
7. C. Kocabaldir, A. Yücel, and C. Kocabaldir, "GIS-Based Multi-Criteria Decision Analysis of Site Selection for Photovoltaic Power Plants in Çanakkale Province", doi: 10.30897/ijgeo.689570.
8. G. Villacreses, G. Gaona, J. Martínez-Gómez, and D. J. Jijón, "Wind farms suitability location using geographical information system (GIS), based on multi-criteria decision making (MCDM) methods: The case of continental Ecuador," *Renew. Energy*, vol. 109, pp. 275–286, 2017, doi: 10.1016/j.renene.2017.03.041.
9. D. Doljak, G. Stanojević, and D. Miljanović, "a Gis-Mcda Based Assessment for Siting Wind Farms and Estimation of the Technical Generation Potential for Wind Power in Serbia," *Int. J. Green Energy*, vol. 18, no. 4, pp. 363–380, 2021, doi: 10.1080/15435075.2020.1865363.
10. B. Sliz-Szkliniarz and J. Vogt, "GIS-based approach for the evaluation of wind energy potential: A case study for the Kujawsko-Pomorskie Voivodeship," *Renew. Sustain. Energy Rev.*, vol. 15, no. 3, pp. 1696–1707, 2011, doi: 10.1016/J.RSER.2010.11.045.
11. M. Piantanakulchai and N. Saengkhaio, "Evaluation of alternatives in transportation planning using multi-stakeholders multi-objectives AHP modeling," *Proc. East. Asia Soc. Transp. Stud.*, no. January 2003, pp. 1613–1628, 2003, [Online]. Available: https://www.researchgate.net/publication/228426663_Evaluation_of_alternatives_in_transportation_planning_using_multi-stakeholders_multi-objectives_AHP_modeling#pf5
12. A. K. Tripathi, S. Ray, M. Aruna, and S. Prasad, "Evaluation of solar PV panel performance under humid atmosphere," *Mater. Today Proc.*, vol. 45, pp. 5916–5920, 2020, doi: 10.1016/j.matpr.2020.08.775.
13. A. H. Nebey, B. Z. Taye, and T. G. Workineh, "Site Suitability Analysis of Solar PV Power Generation in South Gondar, Amhara Region," *J. Energy*, vol. 2020, pp. 1–15, 2020, doi: 10.1155/2020/3519257.

14. J. R. S. Doorga, S. D. D. V. Rughooputh, and R. Boojhawon, "Multi-criteria GIS-based modelling technique for identifying potential solar farm sites: A case study in Mauritius," *Renew. Energy*, pp. 1201–1219, Apr. 2019, doi: 10.1016/J.RENENE.2018.08.105.
15. H. E. Colak, T. Memisoglu, and Y. Gercek, "Optimal site selection for solar photovoltaic (PV) power plants using GIS and AHP: A case study of Malatya Province, Turkey," *Renew. Energy*, vol. 149, pp. 565–576, Apr. 2020, doi: 10.1016/J.RENENE.2019.12.078.
16. B. Roscher, P. Mortimer, R. Schelenz, G. Jacobs, and A. Baseer, "Optimizing a wind farm layout considering access roads," *J. Phys. Conf. Ser.*, vol. 1618, no. 4, 2020, doi: 10.1088/1742-6596/1618/4/042014.

Disclaimer/Publisher's Note: The statements, opinions and data contained in all publications are solely those of the individual author(s) and contributor(s) and not of MDPI and/or the editor(s). MDPI and/or the editor(s) disclaim responsibility for any injury to people or property resulting from any ideas, methods, instructions or products referred to in the content.